Nonclassical Shallow Water Flows

CARINA M. EDWARDS[1], S.D. HOWISON[1*], H. OCKENDON[1],
AND J.R. OCKENDON[1]
[1]Oxford Centre for Industrial and Applied Mathematics,
Mathematical Institute, University of Oxford,
24-29 St. Giles', Oxford, OX1 3LB, UK.

March 20, 2007

Abstract

This paper deals with violent discontinuities in shallow water flows with large Froude number F.

On a horizontal base, the paradigm problem is that of the impact of two fluid layers in situations where the flow can be modelled as two smooth regions joined by a singularity in the flow field. Within the framework of shallow water theory we show that, over a certain timescale, this discontinuity may be described by a delta-shock, which is a weak solution of the underlying conservation laws in which the depth and mass and momentum fluxes have both delta function and step function components. We also make some conjectures about how this model evolves from the traditional model for jet impacts in which a spout is emitted.

For flows on a sloping base, we show that for flow with an aspect ratio of $O(F^{-2})$ on a base with an $O(1)$ or larger slope, the governing equations admit a new type of discontinuous solution that is also modelled as a delta-shock. The physical manifestation of this discontinuity is a small 'tube' of fluid bounding the flow. The delta-shock conditions for this flow are derived and solved for a point source on an inclined plane. This latter delta-shock framework also sheds light on the evolution of the layer impact on a horizontal base.

Keywords: delta-shock, jet impact, hypercritical flow

1   Introduction

Inviscid, irrotational one-dimensional shallow water flow on a horizontal base is so well studied that it is often used as a paradigm for the theory of hyperbolic systems of partial differential equations. A theoretical difficulty can, however, arise for large Froude number $F = U/\sqrt{gh}$, where U is a typical velocity and h a typical depth. In the 'hypercritical' limit $F \to \infty$, the underlying hyperbolic system becomes

---

*Email address: howison@maths.ox.ac.uk

degenerate in the sense that its characteristics coincide, even though they remain real.

From a practical point of view, the typical scenario for discontinuous shallow water flows is that of regions of smooth flow separated by bores, or hydraulic jumps, at which Rankine–Hugoniot conditions for the conservation of mass and momentum (but not energy) are applied. However, this model usually assumes implicitly that $F = O(1)$. What can happen when $F \gg 1$ is typified by two well-known problems for the shallow water model

$$\frac{\partial \eta}{\partial t} + \frac{\partial (u\eta)}{\partial x} = 0, \qquad (1.1)$$

$$\frac{\partial u}{\partial t} + u\frac{\partial u}{\partial x} + \frac{1}{F^2}\frac{\partial \eta}{\partial x} = 0, \qquad (1.2)$$

where the depth $\eta(x,t)$ and horizontal velocity $u(x,t)$ have been made dimensionless with h, U respectively, the horizontal distance x has been made dimensionless with some wavelength $L \gg h$, and t with L/U.

The first problem we consider is the piston problem in which the fluid is initially at rest with $\eta = 1$ in $x > 0$, and $u = 1$ at $x = t$ for $t > 0$. The resulting flow consists of two uniform regions separated by a discontinuity at $x = x_{\mathrm{b}}(t)$. The Rankine-Hugoniot conditions for conservation of mass and momentum across this bore or shock are

$$\frac{\mathrm{d}x_{\mathrm{b}}(t)}{\mathrm{d}t} = \frac{[u\eta]_-^+}{[\eta]_-^+} = \frac{[\eta u^2 + \frac{1}{2F^2}\eta^2]_-^+}{[u\eta]_-^+}, \qquad (1.3)$$

where $[\,]_-^+$ denotes the difference between the flow ahead of and behind the shock. We find from the explicit solution of (1.1)–(1.3) that the depth behind the shock η_{b} satisfies

$$\eta_{\mathrm{b}}^3 - \eta_{\mathrm{b}}^2 - \eta_{\mathrm{b}}(1 + 2F^2) + 1 = 0 \qquad (1.4)$$

and, as $F \to \infty$, the fluid between the piston and the bore has a depth of $\sqrt{2}F$ and horizontal extent $t/(\sqrt{2}F)$. This situation is reminiscent of shock layers in hypersonic flow (Hayes & Probstein 1966).

The second problem we consider is the Riemann problem in which two liquid layers moving towards each other, in $x \lessgtr 0$ respectively, impact at $x = t = 0$. In particular, for two equal and opposite layers of unit depth and speed, using (1.3) for shocks at $x = \pm Vt$, we find that, in $|x| < Vt$, the velocity is zero and the depth is again $\sqrt{2}F$, while $V \sim 1/(\sqrt{2}F)$ as $F \to \infty$. For more general asymmetric Riemann problems, we will get the scenario of Fig 1(a), where the speed of the water in the column is of $O(1)$.

For either of these problems, it is natural to contrast the predictions of the shallow water model with those of the two-dimensional theory of free surface flows in the absence of gravity; these are only at all easy to analyse in the case of steady motion in some reference frame. The study of such flows suggests that in the fully two-dimensional version of the second problem above, the initial collision of the fluid region produces a jet or 'spout' in which fluid moves upwards with significant
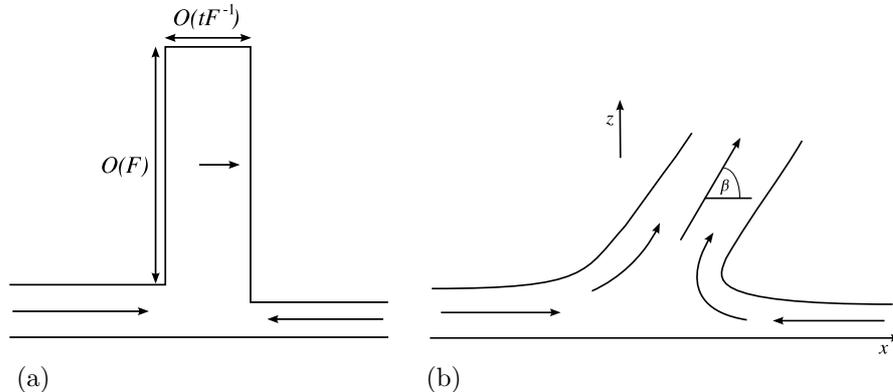
Figure 1: (a) Schematic of the unsteady shallow water solution for the impact of two fluid layers. Two shocks are generated between which the depth is $O(F)$; the width of this region of shocked flow is $O(tF^{-1})$. (b) A classical travelling wave jet impact with $F = \infty$ in which a spout is formed and fluid escapes to infinity; the schematic is drawn in the moving reference frame of the spout.

vertical velocity. Figure 1(b) illustrates the resulting configuration for the second problem above after a sufficient time has elapsed for the flow to be steady in a frame moving with the spout. As discussed in, say, Birkhoff & Zarantonello (1957), and Milne-Thomson (1949), fluid is lost to the spout, which eventually develops into a ballistic trajectory in an inertial frame; we return to the case of symmetric impact, with a vertical spout, below.

One objective in this paper is to try to reconcile these two scenarios and we will begin this in Section 2, where we restrict ourselves to considering flow on a horizontal base. However, the shallow water model with $F = 1$ may also be used to describe the flow of a thin layer over a gently sloping base, provided that the slope is small enough; a famous example is that of flow on a sloping beach as described in Carrier & Greenspan (1958). When the base slope is of order unity then, as long as $F \gg 1$, the fluid will flow uphill at least for some distance. Taking this distance as our length scale we will see in Section 3 that the aspect ratio of the flow δ is such that $\delta \sim O(F^{-2})$. Moreover, the flow is described by the constancy of pressure and Bernoulli's equation and hence the in-plane momentum equation does not involve the layer depth, which is derived subsequently from conservation of mass. Hence such uphill flows can be modelled by uncoupled hyperbolic differential equations (Rienstra 1996). However, it is an everyday observation that when these flows are steady and three-dimensional they cannot survive over long distances, and that they eventually fall back in the form of a concentrated 'mass tube' located near an unknown curve on the substrate (see Figure 2(a)).

Thus the second aim of this paper is to present a theory of such mass tubes viewed as free boundaries for the equations of uphill hypercritical flow, and we will find that this theory will also shed new light on the layer impact problem on a horizontal base.

3
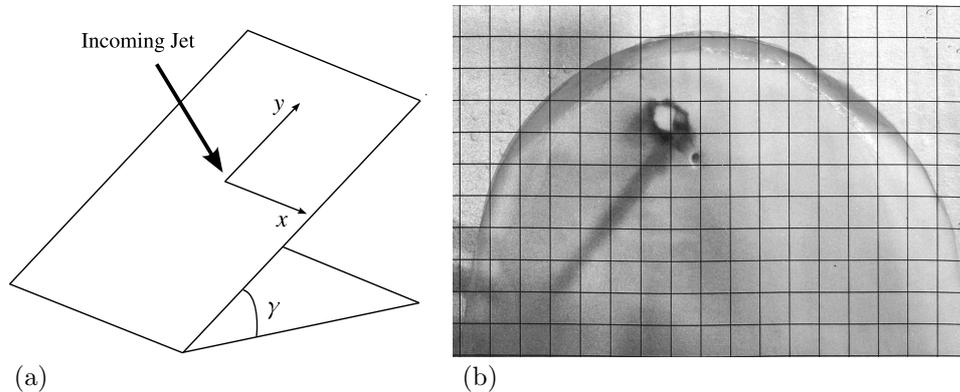
Figure 2: (a) A point source flow on an inclined plane as generated by the normal impact of a jet: the coordinate system used to describe such planar flows in Section 3 is marked. (b) Photograph of the normal impact of a jet on a vertical plane ($\gamma = \pi/2$). The impact of the jet sets up a thin layer flow on the surface which can be idealised as being generated by a point source on the plane. The flow is bounded by a small tube of fluid, which can be distinguished in the photograph as the dark curve. (Photograph, and digital enhancement to bring out the mass tube, by Tom R. Laman.)

2 Flows on a horizontal base

2.1 Delta-shocks

The two problems described in Section 1 suggest that for a hyperbolic system such as (1.1), (1.2), which is degenerate as $F \to \infty$, we can generalise the concept of a weak solution beyond that of one in which u, η are smooth except for jump discontinuities at which (1.3) are satisfied. The solutions of these problems suggest that hypercritical flows might be modelled as solutions of the uncoupled degenerate system obtained by letting $F \to \infty$ in (1.1), (1.2). These equations can be written in conservation form as

$$\frac{\partial(\eta u)}{\partial t} + \frac{\partial(\eta u^2)}{\partial x} = 0, \quad \frac{\partial \eta}{\partial t} + \frac{\partial(u \eta)}{\partial x} = 0 \tag{2.1}$$

as long as we allow u and η to have delta-function behaviour as well as jumps at their singularities. Such a *delta-shock* theory has been developed rigorously in Bouchut (1994), Keyfitz (1999), Li (2001), Li, Zhang & Yang (1998), Yang (1999), and here we will only be concerned with the practicalities of the theory which can be described using ad hoc expansions for the variables. In particular, we avoid the technicalities of the precise definition of products of distributions. We also note that an effective computational algorithm for (2.1) has been proposed in LeVeque (2004) that is capable of predicting profiles such as that shown schematically in Figure 1(a).

4

Assuming a delta-shock at $x = x_\mathrm{s}(t)$ we write

$$\eta = \eta_\mathrm{s}(t)\delta(x - x_\mathrm{s}(t)) + (\eta_\mathrm{r}(x,t) - \eta_\mathrm{l}(x,t))\mathcal{H}(x - x_\mathrm{s}(t)) + \eta_\mathrm{l}(x,t), \qquad (2.2)$$

$$\eta u = M_\mathrm{s}(t)\delta(x - x_\mathrm{s}(t)) + (\eta_\mathrm{r}(x,t)u_\mathrm{r}(x,t) - \eta_\mathrm{l}(x,t)u_\mathrm{l}(x,t))\mathcal{H}(x - x_\mathrm{s}(t))$$
$$+ \eta_\mathrm{l}(x,t)u_\mathrm{l}(x,t), \qquad (2.3)$$

and

$$\eta u^2 = E_\mathrm{s}(t)\delta(x - x_\mathrm{s}(t)) + (\eta_\mathrm{r}(x,t)u_\mathrm{r}^2(x,t) - \eta_\mathrm{l}u_\mathrm{l}^2(x,t))\mathcal{H}(x - x_\mathrm{s}(t))$$
$$+ \eta_\mathrm{l}(x,t)u_\mathrm{l}^2(x,t), \qquad (2.4)$$

where $\delta(\cdot)$ and $\mathcal{H}(\cdot)$ are the delta and Heaviside functions respectively. Since the degenerate shallow water system (2.1) is easily solved by the method of characteristics the functions $u_\mathrm{l,r}$ and $\eta_\mathrm{l,r}$ are assumed to be known continuous solutions of (2.1) in $x < x_\mathrm{s}(t)$ and $x > x_\mathrm{s}(t)$ respectively; we will shortly give an a posteriori justification of this assumption for a specific flow configuration.

The functions $\eta_\mathrm{s}(t)$, $M_\mathrm{s}(t)$, $E_\mathrm{s}(t)$ and $x_\mathrm{s}(t)$ are unknown, and the first three quantities can be interpreted as the amount of mass that has been absorbed into the delta-shock at time t, the momentum of this mass $\eta_\mathrm{s}(t)$ when transported at speed $\dot{x}_\mathrm{s}(t)$ and twice the kinetic energy of this absorbed mass respectively. Substituting (2.2)–(2.4) into the governing equations (2.1) then gives, to lowest order as $F \to \infty$,

$$\frac{\mathrm{d}\eta_\mathrm{s}}{\mathrm{d}t}\delta(x - x_\mathrm{s}(t)) - \eta_\mathrm{s}\frac{\mathrm{d}x_\mathrm{s}}{\mathrm{d}t}\delta'(x - x_\mathrm{s}(t)) - (\eta_\mathrm{r}(x,t) - \eta_\mathrm{l}(x,t))\frac{\mathrm{d}x_\mathrm{s}}{\mathrm{d}t}\delta(x - x_\mathrm{s}(t))$$
$$+ M_\mathrm{s}\delta'(x - x_\mathrm{s}(t)) + (\eta_\mathrm{r}(x,t)u_\mathrm{r}(x,t) - \eta_\mathrm{l}(x,t)u_\mathrm{l}(x,t))\delta(x - x_\mathrm{s}(t)) = 0 \quad (2.5)$$

and

$$\frac{\mathrm{d}M_\mathrm{s}}{\mathrm{d}t}\delta(x - x_\mathrm{s}(t)) - M_\mathrm{s}\frac{\mathrm{d}x_\mathrm{s}}{\mathrm{d}t}\delta'(x - x_\mathrm{s}(t))$$
$$- (\eta_\mathrm{r}(x,t)u_\mathrm{r}(x,t) - \eta_\mathrm{l}(x,t)u_\mathrm{l}(x,t))\frac{\mathrm{d}x_\mathrm{s}}{\mathrm{d}t}\delta(x - x_\mathrm{s}(t)) + E_\mathrm{s}\delta'(x - x_\mathrm{s}(t))$$
$$+ (\eta_\mathrm{r}(x,t)u_\mathrm{r}^2(x,t) - \eta_\mathrm{l}(x,t)u_\mathrm{l}^2(x,t))\delta(x - x_\mathrm{s}(t)) = 0. \quad (2.6)$$

Equating coefficients of δ and δ' in (2.5)–(2.6) we obtain the *delta-shock conditions*

$$M_\mathrm{s} = \eta_\mathrm{s}\frac{\mathrm{d}x_\mathrm{s}}{\mathrm{d}t}, \qquad (2.7)$$

$$\frac{\mathrm{d}\eta_\mathrm{s}}{\mathrm{d}t} = [\eta]_-^+\frac{\mathrm{d}x_\mathrm{s}}{\mathrm{d}t} - [\eta u]_-^+, \qquad (2.8)$$

$$E_\mathrm{s} = M_\mathrm{s}\frac{\mathrm{d}x_\mathrm{s}}{\mathrm{d}t}, \qquad (2.9)$$

$$\frac{\mathrm{d}M_\mathrm{s}}{\mathrm{d}t} = [\eta u]_-^+\frac{\mathrm{d}x_\mathrm{s}}{\mathrm{d}t} - [\eta u^2]_-^+, \qquad (2.10)$$

where, as before, $u^\pm$, $\eta^\pm$ are the values of $u_\mathrm{r,l}$ and $\eta_\mathrm{r,l}$ evaluated either side of the discontinuity. To find the delta-shock position $x_\mathrm{s}(t)$ we must now solve the

5

four dimensional system of differential equations (2.7)–(2.10) along with the field equations instead of the traditional Rankine–Hugoniot shock conditions (1.3).

In order to give further confidence that (2.1) and (2.7)–(2.10) provides the correct scenario within which to solve the hypercritical shallow water equations, let us consider the solution of a smooth initial value problem for η, u rather than the initially discontinuous problems of Section 1. Suppose, for example, that

$$\eta(x,0) \; = \; 1, \quad u(x,0) \; = \; 1 + \cos x. \tag{2.11}$$

Then the solution for u is, for $0 \leq t < 1$,

$$u(x,t) \; = \; 1 + \cos s \quad \text{where} \quad x \; = \; t(1 + \cos s) + s. \tag{2.12}$$

This is the leading-order term in a regular expansion of (1.2) for $F \gg 1$. From (1.1)

$$\eta(x,t) \; = \; \frac{1}{1 - t \sin s}, \tag{2.13}$$

and both $\partial u/\partial x$ and η first become infinite as $t \uparrow 1$ at $s = \pi/2$, $x = 1 + \pi/2$. In the absence of any jump discontinuities, the solutions (2.12), (2.13) are as shown in Figure 3. Moreover, it is impossible to find a traditional weak formulation for $t > 1$ in which u and η each have a single jump discontinuity.

We can also note that in the region near $t = 1$, $x = 1 + \pi/2$ and in particular $|s - \pi/2| = O(\epsilon)$ for some $\epsilon \ll 1$, we can set

$$u \; = \; 1 + \epsilon \hat{u}, \;\; t \; = \; 1 + \epsilon^2 \tau, \;\; \eta \; = \; \epsilon^{-2} \hat{\eta} \tag{2.14}$$

and focus on a region close to the characteristic $x = t + \pi/2$ by writing

$$x - t - \pi/2 \; = \; \epsilon^3 \xi. \tag{2.15}$$

When we substitute these scalings, the original system (1.1), (1.2) becomes

$$\frac{\partial \hat{u}}{\partial \tau} + \hat{u} \frac{\partial \hat{u}}{\partial \xi} + \frac{1}{F^2 \epsilon^4} \frac{\partial \hat{\eta}}{\partial \xi} \; = \; 0, \tag{2.16}$$

$$\frac{\partial \hat{\eta}}{\partial \tau} + \frac{\partial(\hat{u}\hat{\eta})}{\partial \xi} \; = \; 0. \tag{2.17}$$

Hence by choosing $\epsilon = F^{-1/2}$, we return to the full shallow water model no matter how large F is. From (2.12), (2.13), suitable matching conditions as $\tau \to -\infty$ are

$$\hat{u} \sim -\zeta \quad \text{and} \quad \hat{\eta} \sim \frac{2}{\zeta^2 - 2\tau}, \tag{2.18}$$

where ζ satisfies the equation

$$\zeta^3 - 6\tau\zeta - 6\xi \; = \; 0. \tag{2.19}$$

6
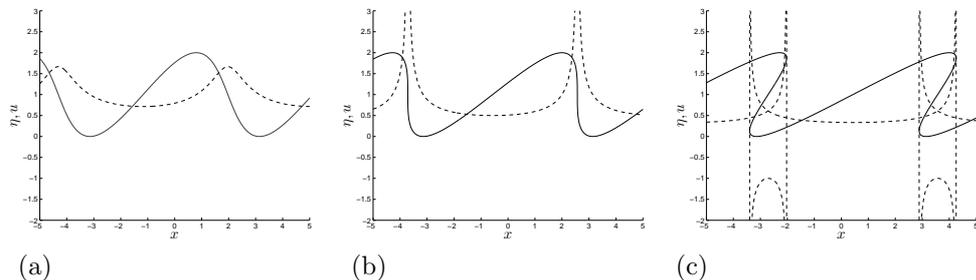
Figure 3: The depth η (dashed line) and velocity u (solid line) profiles (2.12), (2.13) at: (a) $t = 0.4$, (b) $t = 1$, (c) $t = 2$.

Hence

$$\zeta = (3\xi + \sqrt{9\xi^2 - 8\tau^3})^{\frac{1}{3}} + (3\xi - \sqrt{9\xi^2 - 8\tau^3})^{\frac{1}{3}}. \qquad (2.20)$$

A better appreciation of this scenario is gained by comparison with accurate computation of the solution of (1.1), (1.2) subject to (2.11) for $F = 30$. These calculations, kindly performed by P.J. Dellar, are shown in Figure 4. They clearly reveal the emergence of a liquid column bounded by two closely spaced shocks, giving us confidence that we are witnessing the birth of what would become a delta-shock in the limit as $F \to \infty$. For finite F, the shallow water equations (1.1), (1.2) remain non-degenerate as a hyperbolic system and the numerical solutions were obtained using finite volume techniques for hyperbolic systems, the local Lax–Friedrichs or Rusanov (1961) scheme, and its second order extension by Kurganov & Tadmor (2000). Neither scheme requires the solution of the Riemann problem, only the determination of the fluxes as functions of the conserved variables η and ηu, and a bound on the maximum wave speed, taken as $|u| + \sqrt{\eta}/F$. Both schemes lead to systems of ODEs for cell-averaged quantities that were integrated in time using the second order, total variation diminishing, Runge–Kutta method of Shu & Osher (1989). The second order extension gave no noticeable improvement for the very fine grid of 16384 points used in these computations.

We must add that, as shown in Chen & Liu (2003), and Yang (1999), it is necessary to impose an additional selection criterion in order to determine the shock speed uniquely from the delta-shock conditions, just as for traditional Rankine–Hugoniot shocks. We may either invoke causality, which requires that there are no outgoing characteristics, or require that energy is lost, which can be shown to be equivalent to the assertion that the 'mass' of the delta-shock $\eta_s(t)$ increases with time. For (2.1) the fact that all the characteristics are incoming has the added effect of decoupling the field equations from the shock conditions (2.7)–(2.10).

2.2 Discontinuities with loss of mass and momentum

As mentioned in the introduction, the traditional model for the zero-gravity impact of two jets of liquid is as depicted in Figure 1(b). This flow is described by the full

7
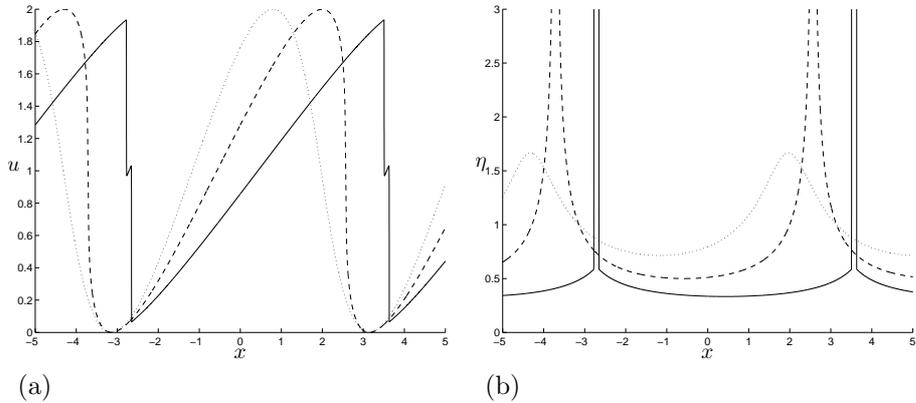
Figure 4: The solution of (1.1), (1.2) subject to (2.11). (Figure provided by P.J. Dellar). (a) The velocity profile u at $t = 0.4$ (dotted line), $t = 1$ (dashed line), $t = 2$ (solid line). (b) The depth η at $t = 0.4$ (dotted line), $t = 1$ (dashed line), $t = 2$ (solid line); the depth attained by the flow at $t = 1$ is 36.5.

Euler equations, including the velocity in the vertical direction, z, with $F = \infty$ as compared with the shallow water model in which the time scale is long enough for the vertical velocity term to be of lower order than the hydrostatic term $F^{-2} \partial \eta / \partial x$ (see (1.2)). In a frame of reference moving with the spout root, the flow is a steady Helmholtz flow. Hence we can use conservation of mass and momentum, and the Bernoulli condition on the free streamlines, to find the spout root position $x_{\mathrm{sp}}(t)$, spout inclination β (measured from the positive x-axis in the moving frame), spout thickness η_{sp} and the velocity along the spout U_{sp} as

$$\frac{\mathrm{d}x_{\mathrm{sp}}}{\mathrm{d}t} = \frac{u^+ + u^-}{2}, \tag{2.21}$$

$$\eta_{\mathrm{sp}} = \eta^+ + \eta^-, \tag{2.22}$$

$$\cos\beta = \frac{\eta^- - \eta^+}{\eta^+ + \eta^-}, \tag{2.23}$$

and

$$U_{\mathrm{sp}} = \frac{u^- - u^+}{2}, \tag{2.24}$$

where, as before, $u^\pm$ and $\eta^\pm$ are the values of the outer flow on either side of the spout. Even when the outer flow is unsteady on the timescale of L/U where $L \gg h$, in a frame of reference moving with the spout the local flow is steady to lowest order and so (2.21)–(2.23) still determine the spout geometry as in Figure 1(b).

This leads us to consider an alternative approach to modelling a singularity through which mass and momentum as well as energy are lost into the z-dimension; we will do this in the spirit of the theory of weak solutions of the outer conservation

8

laws. Indeed, in Yarin & Weiss (1995), the concept of a 'kinematic discontinuity' was introduced as a model for a splash crown formed by a droplet impact, which locally has the structure of a spout. This kinematic discontinuity is described by introducing sinks into the conservation laws so as to model a spout in which both mass and momentum are lost. Thus the flow is modelled by

$$\frac{\partial \eta}{\partial t} + \frac{\partial (\eta u)}{\partial x} = -M_{\text{loss}}(t)\delta(x - x_{\text{sp}}(t)), \tag{2.25}$$

$$\frac{\partial (\eta u)}{\partial t} + \frac{\partial (\eta u^2)}{\partial x} = -E_{\text{loss}}(t)\delta(x - x_{\text{sp}}(t)), \tag{2.26}$$

where M_{loss}, E_{loss} and the spout location x_{sp} are unknown functions of time.

Integrating (2.25), (2.26) across the discontinuity gives that

$$-M_{\text{loss}} = [\eta u]_-^+ - [\eta]_-^+ \frac{\mathrm{d}x_{\text{sp}}}{\mathrm{d}t}, \tag{2.27}$$

$$-E_{\text{loss}} = [\eta u^2]_-^+ - [\eta u]_-^+ \frac{\mathrm{d}x_{\text{sp}}}{\mathrm{d}t}, \tag{2.28}$$

and the obvious way to close the system is to assume that the discontinuity structure is a spout with $\mathrm{d}x_{\text{sp}}/\mathrm{d}t$ being determined by (2.21). A consequence of this assumption is that, relative to an inertial frame, the mass and momentum conditions for the spout flow of Figure 1(b) are, from (2.21)–(2.24),

$$\left[\eta \left(\frac{\mathrm{d}x_{\text{sp}}}{\mathrm{d}t} - u \right) \right]_-^+ = U_{\text{sp}}\eta_{\text{sp}}, \tag{2.29}$$

$$\left[\eta \left(\frac{\mathrm{d}x_{\text{sp}}}{\mathrm{d}t} - u \right)^2 \right]_-^+ = -U_{\text{sp}}^2 \eta_{\text{sp}} \cos \beta. \tag{2.30}$$

Hence, for this particular model, $M_{\text{loss}} = U_{\text{sp}}\eta_{\text{sp}}$ and $E_{\text{loss}} - M_{\text{loss}}\mathrm{d}x_{\text{sp}}/\mathrm{d}t = U_{\text{sp}}^2 \eta_{\text{sp}} \cos \beta$, which implies that

$$E_{\text{loss}} = U_{\text{sp}}\eta_{\text{sp}} \left(U_{\text{sp}} \cos \beta + \frac{\mathrm{d}x_{\text{sp}}}{\mathrm{d}t} \right) = M_{\text{loss}}V, \tag{2.31}$$

say, where V is the horizontal velocity in the spout in the inertial frame. The relation (2.31) was proposed by Yarin & Weiss (1995).

The description (2.27), (2.28) can be generalised to more general impacts. For example, if two unequal layers impact and generate a vortex sheet within the jet, as in Curtis & Kelly (1994), the total heads on either side will differ by $H_0(t)$, and then we simply replace (2.21) by

$$\frac{\mathrm{d}x_{sp}}{\mathrm{d}t} = \frac{u^+ + u^-}{2} + \frac{H_0(t)}{(u^- - u^+)}. \tag{2.32}$$

2.3 Examples

Although the two theories described in Sections 2.1, 2.2 lead to models that are different mathematically, their predictions are often very similar. Suppose, for example, that we return to the symmetric problem of the impact of two equal layers of unit depth moving with velocity ± 1. The delta-shock prediction from (2.7)–(2.10) with $\eta_s = M_s = E_s = 0$ at $t = 0$ is that

$$\eta_s = 2t, \quad x_s(t) = 0, \tag{2.33}$$

while (2.21) and (2.27) predicts that

$$x_{sp}(t) = 0 \tag{2.34}$$

and the spout flux is $U_{sp}\eta_{sp} = 2$ corresponding to a mass growth of[1] $2t$.

Asymmetric impact is less easy to analyse but as an example[2] we will consider the impact of a layer in which $u(0,t) = 1/(1-t)$, $\eta(0,t) = 1-t$ on stationary fluid with $\eta = 1$ in $x > 0$ at $t = 0$. The solution of (2.1) is, for $0 < t < 1$,

$$\eta(x,t) = \begin{cases} \frac{1-t}{(1-x)^2}, & x < X(t), \\ 1, & x > X(t), \end{cases} \tag{2.35}$$

$$u(x,t) = \begin{cases} \frac{1-x}{1-t}, & x < X(t), \\ 0, & x > X(t), \end{cases} \tag{2.36}$$

except near $x = X(t)$, which separates the moving and quiescent fluid layers.

When we assume the delta-shock relations (2.7)–(2.10), we find that the coefficient of the mass delta function $\eta_s(t)$ and the position of the shock $X(t) = x_s(t)$ are

$$\eta_s(t) = x_s(t) + \frac{t-1}{1-x_s(t)} + C, \tag{2.37}$$

$$\eta_s(t)\frac{dx_s}{dt} = \ln\left| A\left(\frac{1-x_s(t)}{1-t}\right)\right|, \tag{2.38}$$

where A and C are constants. The initial conditions for the delta-shock are

$$\eta_s(0) = 0 \text{ and } x_s(0) = 0, \tag{2.39}$$

which gives $C = 1$ and, provided the shock velocity is bounded as $t \downarrow 0$, $A = 1$. We eliminate η_s from (2.37) and (2.38) and integrate to give

$$\frac{1}{2}(x_s(t) + 1)^2 + (1-t)\left(\ln\left|\frac{1-x_s(t)}{1-t}\right| + 1\right) - \frac{3}{2} = 0. \tag{2.40}$$

---

[1] It can be shown more generally that the two models will give the same shock position whenever $u^{\pm}, \eta^{\pm}$ are constant with $\eta^+ = \eta^-$, i.e. with spout angle $\beta = \pi/2$.

[2] In Howison, Ockendon & Oliver (2002) this flow was shown to be relevant to the impact of a rectangular impactor on a quiescent layer. The impactor squeezed out fluid into the quiescent layer and the resulting interaction was modelled as a spout.
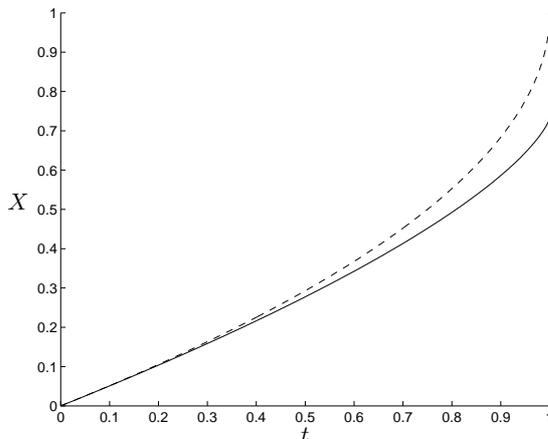
Figure 5: The solid line is the position $x = X(t) = x_{\mathrm{s}}(t)$ of the singularity for the impact problem as predicted by the delta-shock conditions, and given by (2.40). The dashed line is the spout position $x = X(t) = x_{\mathrm{sp}}(t)$ as given by (2.41).

By choosing the solution for $x_{\mathrm{s}}(t)$ that satisfies the causality conditions, this leads to a unique positive solution for $x_{\mathrm{s}}(t)$, and hence for $\eta_{\mathrm{s}}(t)$, which increases with time for $0 < t < 1$.

On the other hand, for a discontinuity with loss and no vortex sheet, the position $X(t) = x_{\mathrm{sp}}$ is given by (2.21) as

$$x_{\mathrm{sp}} = 1 - \sqrt{1 - t}. \tag{2.41}$$

The numerical solution of (2.40) is plotted in Figure 5 alongside the spout root position as given by (2.41). For small times the two solutions only differ by $O(t^3)$, but as mass accumulates in the delta-shock and $\eta_{\mathrm{s}}(t)$ increases, so the delta-shock gains inertia and lags behind the spout, through which mass is continually lost.

2.4 Discussion

We will now make some conjectures concerning the relationship between delta-shocks and discontinuities with loss based on the consideration of the full two-dimensional Euler equations in the (x, z) plane for the symmetric impact problem. Assuming potential flow, in which the velocity potential ϕ has been made dimensionless with Uh, x and z with h and t with h/U, and in the absence of vortex sheets, we have to solve

$$\frac{\partial^2 \phi}{\partial x^2} + \frac{\partial^2 \phi}{\partial z^2} = 0 \quad \text{in } 0 < z < \eta(x, t), \tag{2.42}$$

11
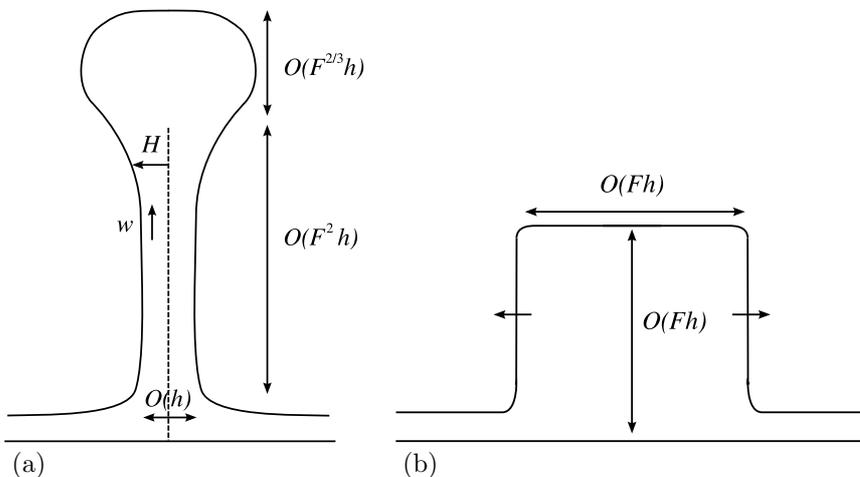
Figure 6: (a) Schematic of flow resulting from the impact of two symmetric jets after a time $t \sim O(F^2)$ in a frame moving with the spout root. (b) Schematic of the flow after the collapse of the fluid column shown in (a); the flow evolves into a connected region bounded by bores.

where η may well be multi-valued, with

$$\frac{\partial \phi}{\partial z} = \frac{\partial \eta}{\partial t} + \frac{\partial \phi}{\partial x}\frac{\partial \eta}{\partial x} \qquad \text{on } z = \eta(x,t), \qquad (2.43)$$

$$\frac{\partial \phi}{\partial t} + \frac{1}{2}|\nabla \phi|^2 + \frac{1}{F^2}\eta = 0 \qquad \text{on } z = \eta(x,t), \qquad (2.44)$$

$$\frac{\partial \phi}{\partial z} = 0 \qquad \text{on } z = 0. \qquad (2.45)$$

The initial conditions are appropriate to the jet collision problem under discussion. Hence, over this timescale, we have an 'unsteady Helmholtz flow' for which, as discussed in King & Needham (1994) even the small time solution is very complicated. Nonetheless, we anticipate that this solution will describe the growth of a vertical column of liquid centred near the initial impact point and that, as $t \to \infty$ with $F = \infty$, the flow will tend to a steady Helmholtz flow in a frame moving with the spout. However, we expect gravitational effects to become important at the apex of the column at dimensional times of $O(U/g)$, i.e. when in (2.42)–(2.45), $t \sim O(F^2)$.

The column may be modelled as a vertical thin jet of water *along* which gravity acts. It occupies the region $-H(z,t) < x < H(z,t)$, $z \gg 1$, in which H and the vertical velocity $w(z,t)$ satisfy

$$\frac{\partial H}{\partial t} + \frac{\partial(wH)}{\partial z} = 0, \qquad (2.46)$$

$$\frac{\partial w}{\partial t} + w\frac{\partial w}{\partial z} = -\frac{1}{F^2}, \qquad (2.47)$$

12

with matching to the Helmholtz flow at the base; see Figure 6(a). Rescaling via $z = F^2 Z$, $t = F^2 T$, we retrieve the same equations with $-1/F^2$ replaced with -1, and with $w = 1$, $H = 1$ at $Z = 0$ for $T > 0$ ($T = 0$ being the initial collision time of the jets on this scale). The solution is

$$w(Z,T) = \sqrt{1 - 2Z}, \qquad H(Z,T) = \frac{1}{\sqrt{1 - 2Z}}, \quad 0 < Z < T - \frac{1}{2}T^2, \quad 0 < T < 1,$$
$$(2.48)$$

the first of which states that the fluid travels ballistically, and the second that as it travels up it 'fills' the space between the fixed curves $x = \pm 1/\sqrt{1 - 2Z}$ (the discontinuity at the top of the jet, $Z = T - \frac{1}{2}T^2$, is a classical shock satisfying the Rankine–Hugoniot conditions for (2.46)).

As the jet nears the top of its trajectory at time $T = 1$, $Z = \frac{1}{2}$, this model gives way to a fully two-dimensional flow, in which the scales are such that the local Froude number is unity. This occurs when $Z = \frac{1}{2} + O(F^{-\frac{4}{3}})$, at which point the lateral extent of the jet $1/\sqrt{1 - 2Z}$ and the vertical scale $\frac{1}{2} - Z$ both translate to the same dimensional lengthscale of $O(F^{\frac{2}{3}}h)$, with the velocities being $O(F^{-\frac{2}{3}}U)$. The relevant timescale is $F^{\frac{4}{3}}h/U$, which is much longer than the time $O(Fh/U)$ that a ballistic particle takes to turn round at the top of its trajectory. This flow is complicated but we conjecture that it leads to the formation of a blob of area $O(F^{\frac{4}{3}}h^2)$, which will be unstable. The geometry may distort dramatically with many changes in connectivity and consequent turbulent dissipation. However, we expect it eventually to collapse into a connected central region of area $O(F^2 h^2)$ bounded by bores at each end (Figure 6(b)). By the end of Section 3, we will be able to present a model for the collapse of the spout but here we simply note that if the collapse does generate such a central core, this core can, when viewed from sufficiently far away, be considered as a delta-shock. We remark that this scenario is qualitatively similar to some of the predictions of the numerical calculations by Anderson, Diver & Peregrine (1990). However, these authors make the cautionary comment that a wild variety of shapes can occur depending on the initial conditions.

3 Uphill shallow water flows

We now return to the modelling of flow over a non-horizontal base, and in particular on an inclined plane as illustrated in Figure 2. If the slope of the base is sufficiently small, specifically of $O(\delta)$, where δ is the aspect ratio of the layer, then, with $F = O(1)$, the flow may be described by the traditional model for shallow water flow on a sloping base (Carrier & Greenspan 1958, Stoker 1957). If, however, the slope of the base exceeds $O(\delta)$ then shallow water flow can only be sustained if it is fast enough that the Froude number is large. In this regime, we show that it is possible for a new type of discontinuity to form, consisting of a small tube of fluid bounding the flow, as seen in Figure 2. Our objective in this section is to find a realistic model for this tube,[3] and we will concentrate on the specific problem of a

---

[3]A geometrically similar phenomenon to this tube can be seen at the edge of *free sheets*, i.e. sheets without a supporting substrate, by, for example, holding a spoon under a tap (Bush &

point source flow, as shown in Figure 2.

Uphill flows have a characteristic length scale independent of the initial conditions, namely the maximum distance the fluid can travel up the plane under the action of gravity, i.e. $U^2/2g\sin\gamma$, where γ is the slope of the plane. Within the framework (2.42)–(2.45), and using the notation of Figure 2, it is now more appropriate to scale the horizontal and uphill distances x and y with[4] $L = U^2/g\sin\gamma$, the potential with UL, the time with L/U and z, the distance perpendicular to the plane, with h. Then we obtain

$$\frac{\partial^2\phi}{\partial z^2} + \delta^2\left(\frac{\partial^2\phi}{\partial x^2} + \frac{\partial^2\phi}{\partial y^2}\right) = 0, \tag{3.1}$$

with

$$\frac{\partial\phi}{\partial z} = \delta^2\left(\frac{\partial\eta}{\partial t} + \frac{\partial\phi}{\partial x}\frac{\partial\eta}{\partial x} + \frac{\partial\phi}{\partial y}\frac{\partial\eta}{\partial y}\right) \tag{3.2}$$

and

$$\frac{1}{2}\left(\frac{\partial\phi}{\partial z}\right)^2 + \delta^2\left(\frac{\partial\phi}{\partial t} + \frac{1}{2}\left(\frac{\partial\phi}{\partial x}\right)^2 + \frac{1}{2}\left(\frac{\partial\phi}{\partial y}\right)^2 + y - \frac{1}{2}\right) + \delta^3(\eta - \eta_0)\cot\gamma = 0 \tag{3.3}$$

on $z = \eta(x,y)$, where η_0 is a reference level, and

$$\frac{\partial\phi}{\partial z} = 0 \tag{3.4}$$

on $z = 0$, where $\delta = h/L = \sin\gamma/F^2 \ll 1$.

We will consider the steady problem of a point source with no directivity at $x = y = 0$, as shown in Figure 2. To lowest order we see that $\phi \sim \phi(x,y) + O(\delta^2)$ where

$$\frac{1}{2}\left(\frac{\partial\phi}{\partial x}\right)^2 + \frac{1}{2}\left(\frac{\partial\phi}{\partial y}\right)^2 = \frac{1}{2} - y, \tag{3.5}$$

(conservation of energy) and then mass conservation is expressed as

$$\frac{\partial}{\partial x}\left(\eta\frac{\partial\phi}{\partial x}\right) + \frac{\partial}{\partial y}\left(\eta\frac{\partial\phi}{\partial y}\right) = 0. \tag{3.6}$$

Equations (3.5) and (3.6) may be written in conservation form as

$$\nabla\cdot(\eta\mathbf{u}) = 0, \tag{3.7}$$
$$\nabla\cdot(\eta u\mathbf{u}) = 0, \tag{3.8}$$
$$\nabla\cdot(\eta v\mathbf{u}) = -\eta \tag{3.9}$$

Hasha 2004, Clark & Dombrowski 1971, Taylor 1959, Taylor 1960, Taylor & Howarth 1959). In these flows it is surface tension that generates and sustains the tube.

[4]For arithmetic convenience we take L to be twice the maximum distance that the fluid can travel up the plane.

where we have introduced $u = \partial\phi/\partial x$ and $v = \partial\phi/\partial y$, and $\nabla = (\partial/\partial x, \partial/\partial y)$.

We note that this model can be generalised to hypercritical flows over curved surfaces as in Rienstra (1996); on a curved surface ∇ is interpreted as the surface gradient operator while (3.8)–(3.9) become

$$\nabla \cdot (\eta \mathbf{u} \otimes \mathbf{u}) = -\eta \mathbf{k} \tag{3.10}$$

where $\mathbf{a} \otimes \mathbf{b}$ is the tensor product of the vectors $\mathbf{a}$ and $\mathbf{b}$, and $\mathbf{k}$ is the unit vertical vector. Note that in this case we take L as the radius of curvature of the surface. Care has to be taken to ensure that the layer does not separate from the substrate as it is now possible for the pressure at the bottom of the fluid layer to become negative. This occurs when the centrifugal force induced by the curvature of the surface overcomes gravity, i.e. when $|\mathbf{u}|^2 \kappa > \mathbf{k} \cdot \mathbf{n}$ where κ is the normal curvature of the surface in the direction $\mathbf{u}$ and $\mathbf{n}$ is the unit normal of the surface.

The eikonal equation (3.5) may be solved by Charpit's method. The characteristics, which are the particle paths, are parametrised by τ as

$$x = p_0 \tau, \tag{3.11}$$

$$y = q_0 \tau - \frac{\tau^2}{2}, \tag{3.12}$$

where p_0, q_0 are the values of $\partial\phi/\partial x$, $\partial\phi/\partial y$ on each particle path at $\tau = 0$. For the point source we take $p_0 = \sin\theta$, $q_0 = \cos\theta$, where θ parametrises the streamlines and $\theta = 0$ on $x = 0, y > 0$; (3.11), (3.12) then give the velocity as

$$\frac{\partial\phi}{\partial x} = \sin\theta, \tag{3.13}$$

$$\frac{\partial\phi}{\partial y} = \cos\theta - \tau. \tag{3.14}$$

Equation (3.6) for η can be rewritten as

$$\frac{\mathrm{d}}{\mathrm{d}\tau}(\eta J) = 0 \tag{3.15}$$

where $J = \partial(x, y)/\partial(\tau, \theta)$, and hence η is given by[5]

$$\eta = \frac{1}{\tau(1 - \tau\cos\theta)}. \tag{3.16}$$

Figure 7 shows the particle paths and their envelope or caustic $y = \frac{1}{2} - \frac{1}{2}x^2$. On the caustic $J = 0$, and the depth is infinite, which motivates the introduction of a generalised solution in the spirit of Section 2.1.

Recalling that what we see in Figure 2 is a fast thin sheet bounded by a small tube of fluid with no fluid beyond it, we will now idealise the tube as a line condensation to which mass and momentum are continually added from the sheet, and

---

[5]The constant of integration in (3.16) can be taken as unity by scaling the velocity U appropriately in terms of the flux.
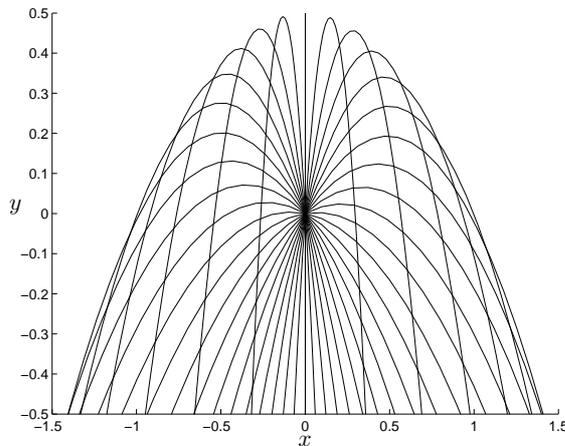
Figure 7: The characteristics, or particle paths, for a point source flow on an inclined plane.

along which there are mass and momentum fluxes. It forms a bounding discontinuity in the flow whose position must be determined by appropriate free boundary conditions. In the next section, we will use the idea of delta-shocks for the degenerate hyperbolic system (3.7)–(3.8) to determine the position of this tube, showing that the presence of the tube causes a significant decrease in the maximum distance up the slope attained by the layer as it flows uphill compared with the distance $U^2/2g\sin\gamma$ of the apex of the caustic.

3.1 Modelling a mass tube as a delta-shock

The equations to be solved are (3.7)–(3.9). We write the mass tube Γ as $y = y_{\mathrm{m}}(x)$. We also assume that the surface is dry in $y > y_{\mathrm{m}}(x)$. Referring to Figure 8, we define a unit tangent $\mathbf{t}_{\mathrm{m}}$ in the direction of the flow in the mass tube, and a normal $\mathbf{n}_{\mathrm{m}}$ into the tube from the sheet, and measure the arc length s along the tube from $x = 0$ in the direction of $\mathbf{t}_{\mathrm{m}}$. We model the mass tube as a delta-shock and introduce a delta function supported on Γ, which we denote by δ_{Γ}, into the film thickness, and into the film mass and momentum fluxes. Thus, following (2.2)–(2.4) we replace η by the distribution

$$A(s)\delta_{\Gamma} + \eta(x, y)\mathcal{H}_{\Gamma}, \tag{3.17}$$

and $\eta\mathbf{u}$, $\eta u\mathbf{u}$ and $\eta v\mathbf{u}$ by the distributions

$$M(s)\mathbf{t}_{\mathrm{m}}\delta_{\Gamma} + \eta\mathbf{u}\mathcal{H}_{\Gamma}, \tag{3.18}$$

$$E(s)(\mathbf{t}_{\mathrm{m}} \cdot \mathbf{e}_x)\mathbf{t}_{\mathrm{m}}\delta_{\Gamma} + \eta u\mathbf{u}\mathcal{H}_{\Gamma}, \tag{3.19}$$

$$E(s)(\mathbf{t}_{\mathrm{m}} \cdot \mathbf{e}_y)\mathbf{t}_{\mathrm{m}}\delta_{\Gamma} + \eta v\mathbf{u}\mathcal{H}_{\Gamma}, \tag{3.20}$$

respectively, where $\mathcal{H}_{\Gamma}$ is a Heaviside function that is unity in $y < y_{\mathrm{m}}(x)$, and $\mathbf{e}_{x,y}$ are unit vectors in the x, y directions respectively, and (3.18)–(3.20) are defined in a

16
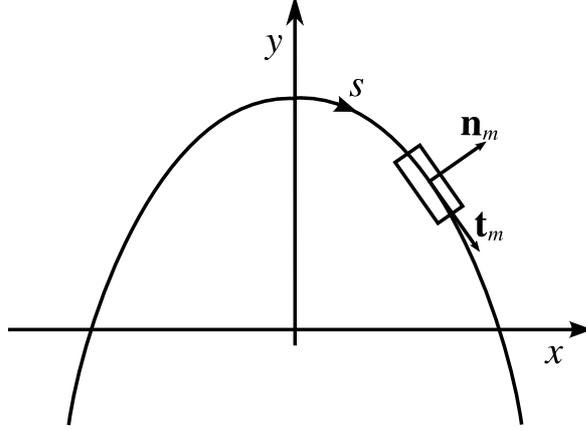
Figure 8: A schematic of the bounding tube of fluid $y = y_\mathrm{m}(x)$ generated by a point source flow on a base with an $O(1)$ slope.

distributional sense by their scalar-product action on a vector valued test function. The weight $A(s)$ can be interpreted as the area of cross section of the tube, while $M(s)$ and $E(s)$ can be interpreted as the mass and momentum fluxes along the tube respectively, and so $M^2 = EA$.

Using the expressions (3.17)–(3.20), the delta-shock conditions for this steady flow may be derived rigorously by a measure theoretic argument. However, we can use a similar argument to that of Section 2.1 and substitute (3.17)–(3.20) into (3.7)–(3.9). Interpreting the divergence of (3.18)–(3.20) in a distributional sense this gives the delta-shock conditions as

$$\frac{\mathrm{d}M}{\mathrm{d}s} = \eta^-(\mathbf{u}^- \cdot \mathbf{n}_\mathrm{m}), \qquad (3.21)$$

$$\frac{\mathrm{d}(E\mathbf{t}_\mathrm{m})}{\mathrm{d}s} = \eta^-\mathbf{u}^-(\mathbf{u}^- \cdot \mathbf{n}_\mathrm{m}) - \frac{M^2}{E}\mathbf{e}_y; \qquad (3.22)$$

here η^- denotes the depth in the sheet evaluated at $y = y \uparrow y_\mathrm{m}(x)$, with the velocity $\mathbf{u}^-$ similarly defined. The mass conservation equation (3.21) tells us that all the fluid entering the tube is absorbed by it. The momentum equation (3.22) can be expressed in terms of its components in the tangential and normal directions $\mathbf{t}_\mathrm{m}$ and $\mathbf{n}_\mathrm{m}$ as

$$\frac{\mathrm{d}E}{\mathrm{d}s} = \eta^-(\mathbf{u}^- \cdot \mathbf{t}_\mathrm{m})(\mathbf{u}^- \cdot \mathbf{n}_\mathrm{m}) - \frac{M^2}{E}\mathbf{e}_y \cdot \mathbf{t}_\mathrm{m}, \qquad (3.23)$$

$$E\frac{\mathrm{d}\mathbf{t}_\mathrm{m}}{\mathrm{d}s} \cdot \mathbf{n}_\mathrm{m} = \eta^-(\mathbf{u}^- \cdot \mathbf{n}_\mathrm{m})^2 - \frac{M^2}{E}\mathbf{e}_y \cdot \mathbf{n}_\mathrm{m}, \qquad (3.24)$$

where $(\mathrm{d}\mathbf{t}_\mathrm{m}/\mathrm{d}s) \cdot \mathbf{n}_\mathrm{m}$ is the curvature of the tube; in (3.24) the centrifugal force due to the flow down the tube is balanced with the force exerted on the tube by the incoming sheet, and gravity, while (3.23) represents the tangential momentum balance.

17

We remark that if the surface is not planar then we can again use the argument above to derive the delta-shock conditions. In this case we substitute (3.17) and (3.18) into (3.7), and (3.10) but we must also replace $\eta\mathbf{u}\otimes\mathbf{u}$ with

$$E(s)\mathbf{t}_\mathrm{m}\otimes\mathbf{t}_\mathrm{m}\delta_\Gamma + \eta\mathbf{u}\otimes\mathbf{u}\mathcal{H}_\Gamma, \tag{3.25}$$

taking an appropriate distributional definition for the divergence of (3.25). We find that (3.21), (3.22) still describe the position of the singularity, but with $\mathbf{e}_y$ replaced by $\mathbf{k}$. However, the vector $\mathrm{d}(E\mathbf{t}_\mathrm{m})/\mathrm{d}s$ has a component in the direction of the normal to the surface $\mathbf{n}$. Additionally, the gravitational body force $-(M^2/E)\mathbf{k}$ has a component into the surface along $\mathbf{n}$. Thus, we see that if

$$\left(E\frac{\mathrm{d}\mathbf{t}_\mathrm{m}}{\mathrm{d}s} + \frac{M^2}{E}\mathbf{k}\right)\cdot\mathbf{n} \quad < \quad 0 \tag{3.26}$$

then there is a resultant force on the mass tube out of the surface, which may cause it to detach from the surface.

In order to complete the solution for the point source flow we must solve the equations (3.21) and (3.23)–(3.24) with the outer solution being given in terms of the ray variables θ, τ. We thus represent the mass tube by $\tau = \tau_\mathrm{m}(\theta)$. The velocities are $u^- = u(\tau_\mathrm{m}(\theta), \theta)$, $v^- = v(\tau_\mathrm{m}(\theta), \theta)$, and $\eta^- = \eta(\tau_\mathrm{m}(\theta), \theta)$ as given by (3.13), (3.14), (3.16) and we introduce, with a slight abuse of notation, $x_\mathrm{m}(\theta) = \tau_\mathrm{m}\sin\theta$ and $y_\mathrm{m}(\theta) = \tau_\mathrm{m}\cos\theta - \tau_\mathrm{m}^2/2$. Thus, writing $' = \mathrm{d}/\mathrm{d}\theta$

$$\mathbf{t}_\mathrm{m} \quad = \quad \frac{1}{\sqrt{x_\mathrm{m}'^2 + y_\mathrm{m}'^2}}(x_\mathrm{m}', y_\mathrm{m}'), \quad \mathbf{n}_\mathrm{m} = \frac{1}{\sqrt{x_\mathrm{m}'^2 + y_\mathrm{m}'^2}}(-y_\mathrm{m}', x_\mathrm{m}'), \tag{3.27}$$

and the mass tube equations (3.21) and (3.23)–(3.24) may be expressed as

$$M' \quad = \quad \frac{-y_\mathrm{m}'\sin\theta + (\cos\theta - \tau_\mathrm{m})x_\mathrm{m}'}{\tau_\mathrm{m}(1 - \tau_\mathrm{m}\cos\theta)} \quad = \quad 1, \tag{3.28}$$

$$E' \quad = \quad \frac{x_\mathrm{m}'\sin\theta + (\cos\theta - \tau_\mathrm{m})y_\mathrm{m}'}{\sqrt{x_\mathrm{m}'^2 + y_\mathrm{m}'^2}} - \frac{M^2}{E}y_\mathrm{m}', \tag{3.29}$$

$$E\frac{-x_\mathrm{m}''y_\mathrm{m}' + x_\mathrm{m}'y_\mathrm{m}''}{x_\mathrm{m}'^2 + y_\mathrm{m}'^2} \quad = \quad \frac{-y_\mathrm{m}'\sin\theta + (\cos\theta - \tau_\mathrm{m})x_\mathrm{m}'}{\sqrt{x_\mathrm{m}'^2 + y_\mathrm{m}'^2}} - \frac{M^2}{E}x_\mathrm{m}'. \tag{3.30}$$

Assuming that the mass flux is zero at the highest point of the flow, (3.28) has the exact solution $M(\theta) = \theta$, and we need only solve (3.29) and (3.30) for $E(\theta)$ and $\tau_\mathrm{m}(\theta)$.

It would be natural to assume that the highest point of the tube is at the top of the caustic, i.e. at $y = \frac{1}{2}$, but it can be shown via a local expansion that this implies a contradiction. Thus instead we let $\tau_\mathrm{m}(0) = \tau_0$ with τ_0, which is expected to be less than unity, to be determined as part of the local solution. We expand τ_m and E as

$$E \quad \sim \quad m_0\theta^2 + m_1\theta^4 \ldots, \tag{3.31}$$

$$\tau_\mathrm{m} \quad \sim \quad \tau_0 + \tau_1\theta^2 + \ldots , \tag{3.32}$$
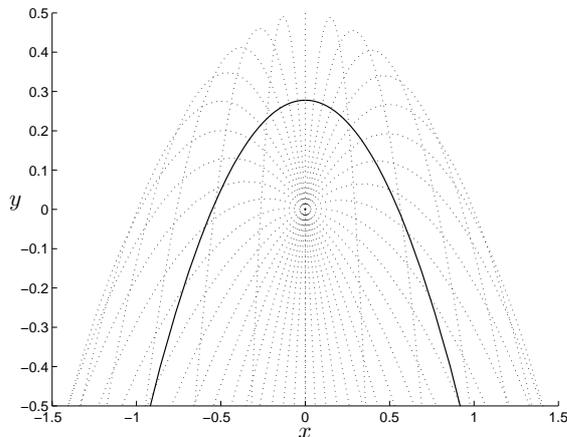
Figure 9: The solid line corresponds to the solution of the mass tube equations (3.28)–(3.30). The dotted lines are the characteristics of the flow as calculated from (3.5). The mass tube is the physical bound for the fluid with the surface dry above it.

for small θ, where the forms of these expansions are determined by the symmetry of the mass tube about $x = 0$ and from a consideration of the possible expansions of (3.29) and (3.30). Equating powers of θ in the expansions of (3.29) and (3.30) we find that $\tau_0 = 1/3$, $m_0 = 1/2$, $\tau_1 = 23/234$ and $m_1 = 5519/109512$. In x, y coordinates this gives the start of the tube as $(0, 5/18)$ rather than $(0, 1/2)$.

We can now use this local solution to provide the initial conditions for solving (3.28)–(3.30) by a fourth–order Runge–Kutta method, and the result is plotted in Figure 9 (incidentally the solution is not a parabola), in which the characteristics on the equation (3.5) are also plotted for comparison. The tube lies below the envelope of characteristics and represents the bounding curve for the fluid with the surface dry above it.

The shape of the mass tube we have calculated is qualitatively similar to the mass tube of Figure 2(a), but calculations based on rough measurements in this kitchen-sink experiment suggest that the rise is about $\frac{1}{3}$ of that predicted by our theory. Viscous drag is a plausible candidate to account for the shortfall, and we briefly consider its effects. We suppose that a jet of radius a impinges normally with speed U on a vertical plate and estimate some orders of magnitude for various properties of the flow. For our experiment U is about 1.8 m s^{-1} and $a = 2 \times 10^{-3} \text{ m}$ with $\nu \sim 10^{-6} \text{ m}^2 \text{ s}^{-1}$; thus at a distance $O(a)$ from the jet the Reynolds number is $Ua/\nu \sim O(10^3)$ and the Froude number is $U/\sqrt{ga} \sim O(10)$. Hence the theory described in this paper applies to this flow. Now we move away from the jet to a radial distance R and suppose that the mean velocity has not changed by an order of magnitude. Then the layer thickness will be $H \sim O(a^2/R)$ and the Froude number will be $U/\sqrt{gH} \sim O(U\sqrt{R/ga^2})$, which is large over the entire range of our experiment. The reduced Reynolds number, which measures the importance

19

of viscosity in the layer, is $UH^2/R\nu \sim O(Ua^4/R^3\nu)$ and when this drops to $O(1)$ then our inviscid theory will no longer apply. For our experiment this happens when R is approximately 2 cm. Hence we expect viscosity to influence the flow appreciably as the mass tube is approached. It would be interesting to perform the experiment for larger values of U and a, with $U/\sqrt{ga}$ held fixed but this proved to be impossible with the simple equipment at hand.

3.2   Implications for horizontal layer impact

We now revisit the symmetric impact problem of Section 2.1 in the light of the discussion above. We recall that, in Section 2.4, we proposed that, over dimensional times of $O(U/g)$, gravity would bring the apex of the vertical spout to rest. Let us therefore consider the possibility of modelling the subsequent effect of gravity as being such as to create an unsteady *horizontal* mass tube as in Figure 6(a) bounding a flow of a sheet up a vertical plane $\gamma = \pi/2$. The corresponding unsteady version of (3.7)–(3.9) for a spout of thickness $2H$ and vertical velocity w in the z direction is as in Section 2.4

$$\frac{\partial H}{\partial t} + \frac{\partial (Hw)}{\partial z} = 0, \tag{3.33}$$

$$\frac{\partial (Hw)}{\partial t} + \frac{\partial (Hw^2)}{\partial z} = -H. \tag{3.34}$$

The mass tube is characterised by a delta-shock at $z = z_{\mathrm{m}}(t)$ whose thickness, mass and momentum are $A(t)$, $M(t)$ and $E(t)$ respectively.

Replacing

$$H \quad \text{by} \quad A\delta(z - z_{\mathrm{m}}) + H\mathcal{H}(z - z_{\mathrm{m}}), \tag{3.35}$$

$$Hw \quad \text{by} \quad M\delta(z - z_{\mathrm{m}}) + Hw\mathcal{H}(z - z_{\mathrm{m}}), \tag{3.36}$$

$$Hw^2 \quad \text{by} \quad E\delta(z - z_{\mathrm{m}}) + Hw^2\mathcal{H}(z - z_{\mathrm{m}}), \tag{3.37}$$

where $\mathcal{H}$ is again the Heaviside function and is unity in $z < z_{\mathrm{m}}$, we find that

$$A\frac{\mathrm{d}z_{\mathrm{m}}}{\mathrm{d}t} = M, \tag{3.38}$$

$$\frac{\mathrm{d}A}{\mathrm{d}t} = H^-\left(w^- - \frac{\mathrm{d}z_{\mathrm{m}}}{\mathrm{d}t}\right), \tag{3.39}$$

$$\frac{\mathrm{d}M}{\mathrm{d}t} = H^-w^-\left(w^- - \frac{\mathrm{d}z_{\mathrm{m}}}{\mathrm{d}t}\right) - A, \tag{3.40}$$

$$M\frac{\mathrm{d}z_{\mathrm{m}}}{\mathrm{d}t} = E, \tag{3.41}$$

where $^-$ denotes the value of a variable as it enters the mass tube. Also the steady flow in the sheet implies from (3.33), (3.34) that

$$w^- = \sqrt{1 - 2z_{\mathrm{m}}}, \quad H^- = \frac{1}{\sqrt{1 - 2z_{\mathrm{m}}}}, \tag{3.42}$$

as derived in Section 2.4. When we choose the origin of time as that at which the spout apex is brought to rest, which is U/g in dimensional variables, the initial conditions are

$$M(0) = 0, \quad A(0) = 0, \quad z_{\mathrm{m}}(0) = \frac{1}{2}. \tag{3.43}$$

The system (3.38)–(3.40) has enough symmetry for us to be able to integrate twice to obtain

$$z_{\mathrm{m}} = \frac{1}{2} - \frac{1}{8}t^2, \quad A = \frac{3}{2}t, \quad M = -\frac{3}{8}t^2. \tag{3.44}$$

This implies that the mass tube descends with one quarter of the acceleration of gravity and hits the base after a fall time twice that taken for the spout apex to reach its apogee. Of course a new model is needed to describe the way in which the mass tube evolves into the expanding, increasingly high aspect ratio central region proposed in Section 2.4. This model will presumably comprise the full Euler equations over the birth of the region on the timescale U/g, but with allowance made for energy dissipation at the edge of the central region.

4   Conclusion

This paper has reviewed the traditional models for the sudden geometrical changes that can sometimes occur in shallow water flows, and has suggested some new models for flows with large Froude number F. When F is of $O(1)$, shallow water flows are well-described by smooth solutions of the equations of shallow water theory, joined by discontinuities whose positions are determined by the traditional Rankine–Hugoniot relations. If, however, F is large, with inertia dominating gravity, then this hyperbolic model becomes nearly degenerate, with its two characteristics coinciding at lowest order. This, in turn, leads to the presence of very strong hydraulic jumps, which may be so close together as to invalidate the shallow water model. This means that new singularities such as delta-shocks or 'discontinuities with mass loss' must be brought into play.

This situation has motivated our investigation into the relative importance of shallow water theory and fully two-dimensional zero-gravity unsteady 'Helmholtz flows' in modelling high-speed shallow flows. These are the only two asymptotic simplifications that can be made in the full equations for the surface gravity waves on a horizontal base: in the shallow water limit, the aspect ratio δ tends to zero before the small gravity limit and in unsteady Helmholtz flows these limits are reversed. However, in any practical problem, F and δ have to be determined as part of the solution and hence we have restricted attention to two case studies.

In Section 2, we have considered the impact of two fast thin sheets flowing horizontally. The predictions of shallow water theory with delta-shocks have been compared with those whose mass loss is incorporated at the discontinuity. While these predictions are in general agreement with each other, neither can describe the detailed temporal evolution of the impact. Hence we have proposed a scenario involving a sequence of

(i) an unsteady Helmholtz flow at very short times;

(ii) classical shallow water theory as the impacting layers move in a vertical spout, with a quasi-steady Helmholtz flow at its base;

(iii) a second unsteady Helmholtz flow at the apex of the spout;

(iv) a downward shallow water flow with a delta-shock;

(v) another, more complicated unsteady Helmholtz flow describing the collapse of the spout;

(vi) a shallow water flow behind a Rankine-Hugoniot shock emitted into the original layer.

In Section 3, we have considered high Froude number flow of a layer on a tilted base. Traditional shallow water theory does not describe such uphill flows but, in steady flow, the solution of the eikonal equation to which the energy equation is equivalent will in general have caustics and the eikonal model breaks down before this caustic is reached. We have proposed a scenario in which the caustic is avoided by the introduction of a condensed mass tube that bounds the flow, this tube having cross-sectional dimension much greater than the layer thickness but much less that the overall flow dimensions. The tube is modelled as a delta-shock in the shallow water equations of motion of the layer in conservation form and the numerical solution for such a delta-shock resulting from a point source flow shows qualitative agreement with crude experimental observations.

Acknowledgements

References

Anderson, A., Diver, D.A. & Peregrine, D.H. (1990) Slender, steep and breaking water waves, *Proc. 5th Internat. Workshop on Water Waves and Floating Bodies. Manchester Univ.*, 8–13.

Birkhoff, G. & Zarantonello, E.H. (1957) *Jets, Wakes and Cavities*, Academic Press, New York.

Bouchut, F. (1994) On zero pressure gas dynamics, *in* 'Advances in Kinetic Theory and Computing', Vol. 22 of *Advances in Mathematics for Applied Sciences*, World Scientific.

Bush, J.W.M. & Hasha, A.E. (2004) On the collision of laminar jets: fluid chains and fishbones, *J. Fluid Mech.*, **511**, 285–310.

Carrier, G.F. & Greenspan, H.P. (1958) Water waves of finite amplitude on a sloping beach, *J. Fluid Mech.*, **4**, 97–109.

Chen, G-Q & Liu, H. (2003) Formation of δ-shocks and vacuum states in the vanishing pressure limit of solutions to the Euler equations for isentropic fluids, *J. Math. Anal.*, **34**, 925–938.

Clark, C.J. & Dombrowski, N. (1971) The dynamics of the rim of a fan spray sheet, *Chem. Eng. Sci.*, **26**, 1949–1952.

Curtis, J.P. & Kelly, R.J. (1994) Circular streamline model of shaped-charge jet and slug formation with asymmetry, *J. Appl. Phys.*, **75**, 7700–7709.

Hayes, W.D. & Probstein, R.F. (1966) *Hypersonic Flow Theory*, Vol. I, Academic Press, New York.

Howison, S.D., Ockendon, J.R. & Oliver, J.M. (2002) Deep- and shallow-water slamming at small and zero deadrise angles, *J. Engrg. Math.*, **42**, 373–388.

Keyfitz, B-L. (1999) Conservation laws, delta shocks and singular shocks, *in* M.Grosser, G.Hörmann, M.Kunzinger & M.Oberguggengerger, eds, 'Nonlinear Theory of Generalized Functions', Research Notes in Mathematics, Chapman and Hall.

King, A.C. & Needham, D.J. (1994) The initial development of a jet caused by fluid, body and free-surface interaction. P art 1. A uniformly accelerating plate, *J. Fluid Mech.*, **268**, 89–101.

Kurganov, A. & Tadmor, E. (2000) New high resolution central schemes for nonlinear conservation laws, *J. Computational Phys.*, **160**, 241–282.

LeVeque, R.J. (2004) The dynamics of pressureless dust clouds and delta waves, *J. Hyperbolic Differ. Equ.*, **1**, 315–327.

Li, J. (2001) Note on the compressible Euler equations with zero temperature, *Appl. Math. Lett.*, **14**, 519–523.

Li, J., Zhang, T. & Yang, S. (1998) *The Two-Dimensional Riemann Problem In Gas Dynamics*, number 98 *in* 'Pitman Monographs and Surveys in Pure and Applied Mathematics', Longman, Scientific and Technical.

Milne-Thomson, L.M. (1949) *Theoretical Hydrodynamics*, Macmillan, London.

Rienstra, S.W. (1996) Thin layer flow along arbitrary curved surfaces, *ZAMM*, **76**, 423–424.

Rusanov, V.V. (1961) Calculation of interaction of non-steady shock waves with obstacles, *J.Comput. Math. Phys. USSR*, **1**, 267–279.

Shu, C.-W. & Osher S.J. (1989) Efficient implementation of essentially non-oscillatory shock capturing schemes II, *J. Comput. Phys.*, **83**, 32–78.

Stoker, J.J. (1957) *Water Waves*, Interscience, New York.

Taylor, G.I. (1959) The dynamics of thin sheets of fluid. III. Disintegration of fluid sheets, *Proc. Roy. Soc. Ser. A*, **253**, 313–321.

Taylor, G.I. (1960) Formation of thin flat sheets of water, *Proc. Roy. Soc. Ser. A*, **259**, 1–17.

Taylor, G.I. & Howarth, L. (1959) The dynamics of thin sheets of fluid. I. Water bells, *Proc. Roy. Soc. Ser. A*, **253**, 289–295.

Yang, H. (1999) Riemann problems for a class of coupled hyperbolic systems of conservation laws, *J. Differential Equations*, **159**, 447–484.

Yarin, A.L. & Weiss, D.A. (1995) Impact of drops on solid surfaces: self-similar capillary waves and splashing as a new type of kinematic discontinuity, *J. Fluid Mech.*, **283**, 141–173.

List of Figures